Heliyon 10 (2024) e33811

Contents lists available at ScienceDirect

Heliyon

journal homepage: www.cell.com/heliyon

Research article

Adsorptive performances and valorization of green synthesized biochar–based activated carbon from banana peel and corn cob composites for the abatement of Cr(VI) from synthetic solutions: Parameters, isotherms, and remediation studies

Hirpha Adugna Areti, Abdisa Jabesa *, Melkiyas Diriba Muleta, Abdi Nemera Emana

Department of Chemical Engineering, Haramaya Institute of Technology, Haramaya University, P. O. Box: 138, Dire Dawa, Ethiopia

ARTICLE INFO

Keywords:
Activated carbon
Adsorption processes
Hexavalent chromium
Isotherm modeling
Wastewater

ABSTRACT

This study intended to remove Cr(VI) from an aqueous synthetic solution employing synthesized biochar adsorbent from a blend of locally sourced banana peel, and corn cob biomass wastes. An equal ratio of the prepared powder was activated with $ZnCl_2$ solution (1:1 wt basis) and carbonized for 2 h at 600 °C. The proximate analysis of the selected BP-CCAC@ZC3 biochar was conducted. Subsequently, its surface area, surface functions, and morphology were examined using BET analysis, FTIR, and SEM techniques, respectively. The proximate analysis of BP–CCAC@ZC3 showed a moisture content of 2.37 ± 0.80 %, an ash content of 8.07 ± 0.75 %, volatile matter of 19.38 ± 2.66 %, and fixed carbon of 70.18 %. It was found that the synthesized BP–CCAC@ZC3 had 432.149 m^2/g of a specific area as per the BET surface area analysis. The highest efficiency for Cr(VI) removal was determined to be 97.92 % through adsorption batch tests using a dose of 0.4 g of BP-CCAC@ZC3, an initial Cr(VI) concentration of 20 mg/L, pH of 2, and 35 min contact time. Likewise, the adsorption process was effectively described by the Langmuir isotherm model, which had a high correlation coefficient (R^2 = 0.9977) and a maximum adsorption capacity of 19.16 mg/g, indicating a monolayer adsorption mechanism. The BP-CCAC@ZC3 biochar exhibited reusability for up to four cycles with only a slight decrease in effectiveness, highlighting its potential for sustainable wastewater treatment. Overall, using corn cob and banana peel composites to synthesize activated carbon with $ZnCl_2$ offers a promising method for effectively removing Cr(VI) containing wastewater.

1. Introduction

The presence of toxic contaminants in water systems has escalated concerns about water quality and hygiene, with substantial impacts on all living organisms. This concern is attributed to rapid urban expansion and industrialization, leading to increased pollution of water bodies and soil.The release of untreated sewage wastewater from various industrial activities, including mining, electroplating, welding, petrochemical production, dyeing, and tanning, poses a significant environmental issue. These industrial

* Corresponding author.
E-mail addresses: hirpa513@gmail.com (H. Adugna Areti), abdisa.j@haramaya.edu.et (A. Jabesa).

https://doi.org/10.1016/j.heliyon.2024.e33811
Received 21 December 2023; Received in revised form 9 June 2024; Accepted 27 June 2024
Available online 28 June 2024

operations release wastewater laden with hazardous and toxic chemicals, exacerbating the degradation and pollution of aquatic ecosystems [1]. The discharge of such pollutants into water bodies raises concerns about the overall health of aquatic ecosystems and emphasizes the need for effective wastewater treatment strategies to mitigate the environmental impact [2]. Chromium is widely recognized as a hazardous element that is commonly found in industrial wastewater in various oxidation states and is often used in a variety of industrial activities [3]. Out of the different oxidation states, Cr(VI) is known for its high level of toxicity and its ability to cause mutations, birth defects, and cancer [4–6]. This type of chromium is easily dissolved in natural environments and poses significant health risks to humans, animals, plants, and microorganisms [4]. Moreover, Cr(VI) is known for its high solubility, mobility, and strong oxidation ability, making it particularly harmful to living organisms [6]. Due to this, both the Environmental Protection Agency (EPA) of the United States and the World Health Organization (WHO) have set rigorous regulations on chromium levels in drinking and wastewater to decrease the long-term health hazards related to its exposure [7–9].

Efforts have been made to remediate Cr(VI) contamination in water sources. Various strategies, including the use of graphene oxide-based adsorption, bioremediation with microbial strains, and the synthesis of nanoparticles, have been explored for the effective removal of Cr(VI) from industrial wastewater [4,7]. Likewise, the biotransformation of Cr(VI) into its less toxic form (i.e., Cr(III)) by certain fungal strains has been reported, indicating a potential avenue for reducing its harmful effects. Generally, the stringent regulations on chromium levels in water, particularly targeting Cr(VI), reflect the grave health and environmental concerns associated with this highly toxic form of the element. Research efforts continue to focus on developing effective remediation strategies to mitigate the risks posed by Cr(VI) contamination in water sources.

In the past few years, different methods for removing Cr(VI) from water/wastewater have been employed. These methods include processes such as adsorption [10], electrochemical reduction, ion exchange, electrocoagulation, electrodialysis [11], and membrane filtration [12]. Despite their limitations, such as reagent consumption and cost, adsorption stands out as a promising technology due to its strong surface interaction [13]. Another studies demonstrated the effectiveness of pectin-based aerogels in adsorbing Pb^{2+} from wastewater, highlighting their potential in water treatment applications [11]. The adsorption process is highly regarded for its practicality, cost-effectiveness, and efficiency in removing trace contaminants. Additionally, it is environmentally sustainable, simple to operate, and easy to regenerate [14]. Fig. 1 describes the mechanism of the adsorption and desorption process proposed by Zaimee et al. [15].

Researchers have demonstrated significant interest in utilizing various fruit peels and agricultural residues, including corn cobs, banana peels, orange peels, sugarcane bagasse, rice straws, and moringa stenopetala seeds, as environmentally friendly adsorbents for the removal of contaminants such as Cr(VI) from water/wastewater [16,17]. These agricultural waste peels have been explored for their adsorption capacities, offering a dual benefit of pollutant removal from wastewater and contributing to waste minimization, recovery, and reuse [18,19]. Studies have shown that fruit peels can serve as effective adsorbents for most of heavy metal pollutants like Cd(II), Cu(II), and Pb(II), optimizing waste removal and enhancing industrial wastewater management [20]. The utilization of waste fruit peels as adsorbents aligns with the principles of a circular economy, where biomass waste is repurposed to create value-added products, contributing to environmental sustainability [21]. Furthermore, the development of adsorbents from biomass waste, such as mango peels and snake fruit seed charcoal, highlights ongoing efforts to create alternative materials with high effectiveness for pollutant removal [22,23]. These initiatives not only address environmental challenges but also offer economic benefits by utilizing waste materials to produce valuable products [24].

In Ethiopia, abundant agricultural biomass presents a promising resource for developing biochar-based adsorbents for water

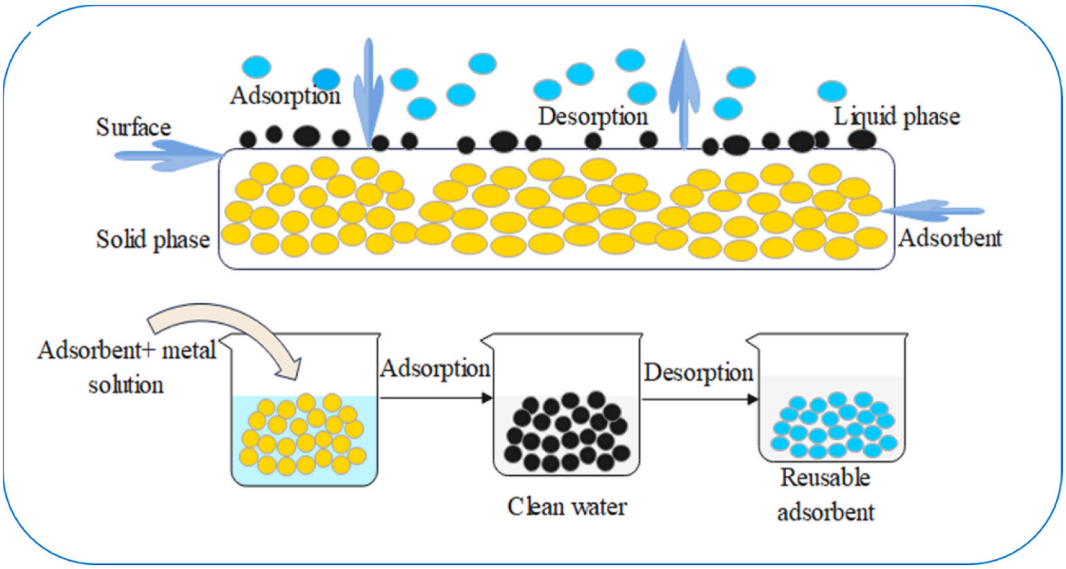

Fig. 1. Heavy metal ions adsorption and desorption mechanisms in wastewater.

treatment, a field still in its early stages locally compared to global trends [25]. Ongoing research aims to harness these resources to improve water quality and develop effective environmental remediation strategies. Specifically, corn cobs and banana peels, which are commonly discarded or burned, causing waste disposal issues and carbon dioxide emissions, offer significant potential [26–28]. Utilizing these residues for sustainable purposes, such as creating adsorbent materials, addresses waste management and environmental protection. Through chemical modification, the combination of corn cobs and banana peels can produce an effective biochar composite for treating sludge wastewater [14]. This approach is not only environmentally friendly but also cost-effective, making it a viable solution for wastewater treatment. The resulting biochar composite is capable of adsorbing and eliminating harmful substances from wastewater efficiently, aligning with the principles of sustainable and green technologies.

$ZnCl_2$ is a promising activator in composite materials, distinguished from common agents such as H_3PO_4, H_2SO_4, and KOH, particularly for enhancing the porosity of carbonaceous materials. Studies suggest it acts as a catalyst during carbonization, promoting the formation of char, aromatic structures, and well-developed pores, leading to a higher specific surface area [29]. For example, research shows the creation of highly porous nanostructures from waste Agave sisalana for supercapacitors, highlighting carbon materials with micropore and mesopore dominance achieved through $ZnCl_2$ activation [30]. Additionally, studies showcase the ability to tailor porosity and magnetic properties of biochar adsorbents from cassava rhizome for dye removal by varying $ZnCl_2$ amounts [31]. Likewise, $ZnCl_2$, along with H_3PO_4 and $FeCl_3$, was used to create activated carbon from chrysanthemum waste for methylene blue adsorption, enhancing the adsorption efficiency [32]. Limited research exists on the effectiveness of $ZnCl_2$-activated corn cob and banana peel biochar composite for removing Cr(VI) from industrial wastewater, a pressing concern in Ethiopia due to chromium contamination. This study proposes such a composite as a sustainable and efficient solution for Cr(VI) removal. Furthermore, the approach promotes waste biomass utilization for wastewater treatment, and can mitigate environmental damage to aquatic ecosystems and soil from Cr(VI) contamination.

This study aimed to create a new biochar composite from corn cob and banana peel activated with $ZnCl_2$ for sustainable Cr(VI) removal through batch tests. It involves a comprehensive analysis of adsorption isotherms and desorption studies to assess the adsorbent's efficiency in addressing Cr(VI) contamination. Furthermore, the study investigates the individual effects of various parameters, such as time, adsorbent dose, initial Cr(VI) concentration, and aqueous solution pH, on the removal of the target pollutant. To characterize the biochar adsorbent, the study used analytical techniques including surface area analysis with Brunauer–Emmett Teller (BET) analysis, morphology analysis with scanning electron microscopy (SEM), and identification of functional groups with Fourier-transform infrared spectroscopy (FTIR). Atomic absorption spectroscopy (AAS) is employed during batch adsorption testing to quantitatively measure Cr(VI) concentrations, and Origin software (version 9.5) was used to generate figures and visualize data for accurate experimental result interpretation.

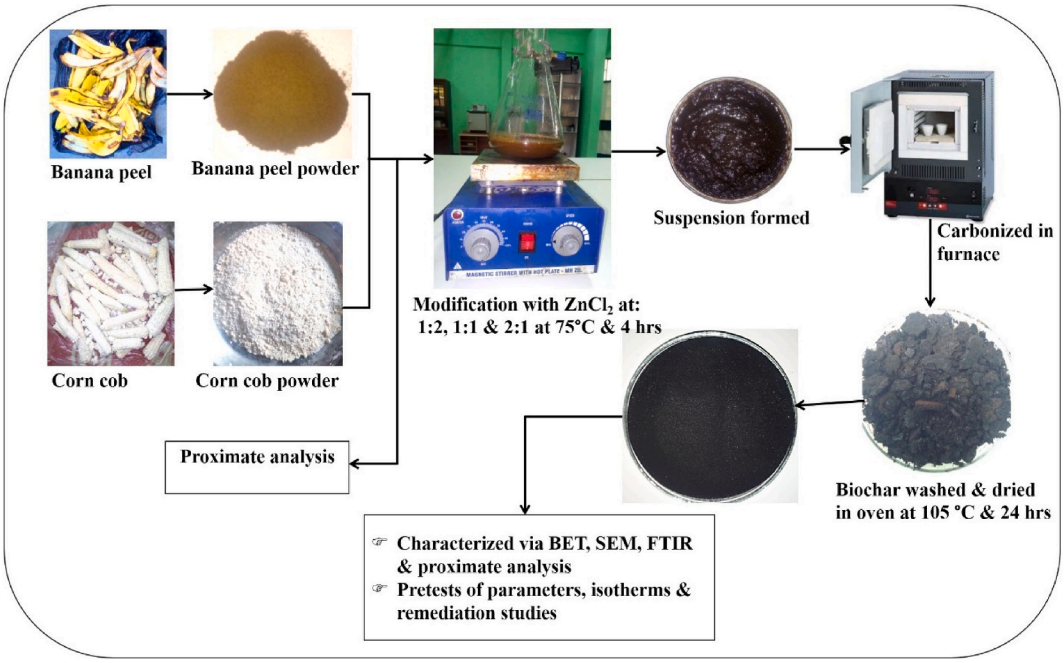

Fig. 2. Steps to modify a biochar preparation from corn cob and banana peel powder and analysis of samples.

2. Materials and methods

2.1. Materials and chemicals used

The materials and chemicals utilized in this study include banana peels, corn cobs, $ZnCl_2$ (99 %, Loba Chemie), $K_2Cr_2O_7$ (99 %, Thermo Fisher Scientific), HCl (35.4 %, Alpha Chemical), NaCl (99.8 %, Rankem Industry), NaOH (98 %, Blulux Laboratories), KBr (98.5 %, Sisco Research Laboratory), and distilled water (DW). The chemicals were of analytical grade, ensuring high purity and minimal interference.

2.2. Experimental procedures for synthesis of an adsorbent

2.2.1. Preparation of raw corn cob and banana peel powder

The samples of corn cob and banana peel were collected from the surroundings of Haramaya University, Ethiopia. Fig. 2 shows the overall steps to prepare and modify a biochar from these two precursors. The collected samples were thoroughly cleaned with DW. According to a previously published method [33], the samples were then chopped into smaller pieces, sun-dried for 72 h, and further dried in an oven at 75 °C for 24 h. Finally, the powdered corn cobs (CCP) and banana peels (BPP) were combined in equal proportions in a 1:1 wt ratio. This mixture has been termed a new precursor (NP) for biochar synthesis and modification.

2.2.2. Surface modification of mixed corn cob and banana peel powder

Chemical modification of dried NP was performed using $ZnCl_2$ as an activating agent, following the procedures described elsewhere [33,34]. First, an amount of $ZnCl_2$ ranging from 20 to 40 g was dissolved in 200 mL of distilled water. Next, 20–40 g of NP was added to the $ZnCl_2$ solution and allowed to soak for 4 h at a temperature of 75 °C, using a hot magnetic stirrer. The mixture was then dried in an oven at 80 °C for 24 h. Following this, the mixture was transferred to a crucible and subjected to carbonization for 1–3 h in a programmable furnace set between 500 and 700 °C to create composite porous biochar. After synthesizing the biochar composites, they were thoroughly washed with a 2 M HCl solution and hot DW to remove any residuals. This washing process continued until the solution reached a neutral pH. The composites were then dried in an oven at 105 °C for 24 h. Once dried, the material was finely ground using a mortar and pestle. Finally, the biochar adsorbent composite, derived from corn cobs and banana peels, was desiccated and prepared for subsequent analysis.

2.3. Biochar adsorbent characterizations

2.3.1. BET surface area analysis

The surface area of the biochar adsorbent was measured using a BET surface analyzer (SA–9600, UK). N_2 adsorption was carried out under vacuum conditions using liquid N_2 at a temperature of 196.5 °C and a degassing of 300 °C with a degassing time of 60 min. The specific area of the adsorbent was determined by analyzing N_2 gas adsorption and desorption isotherms at atmospheric pressure of 700 mmHg [35]. The study investigated the impact of impregnation ratio, contact time, and temperature on the specific BET surface area.

2.3.2. Surface charge analysis

Assessing the surface charge of biochar adsorbents and their ion speciation is crucial for understanding their interaction with aqueous metal ions and other substances [33,36]. To achieve this, five 100 mL volumetric flasks were filled, each with 40 mL of 0.01 M NaCl solution. Then, 0.1 g of biochar adsorbent was added to each flask. The initial pH of the solutions was adjusted within a range of 2–10 using 0.5 M NaOH or 0.5 M HCl. The final pH values were recorded after the solutions were left to reach equilibrium for 24 h. The plot of pH_f versus pH_i where the point it intersects with the axis that passes through zero value of ΔpH was noted as the adsorbent's pHzc. The pH difference (ΔpH) between the initial pH (pH_i) and pH_f was calculated using Eq. (1).

$$\Delta pH = pH_i - pH_f \tag{1}$$

2.3.3. Proximate analysis

Proximate analyses were conducted following the standards established by the American Society for Testing and Materials (ASTM) [37]. Accordingly, ASTM (D2867–09) [38], ASTM (D2866–94), and ASTM (D5832–98) [39] standards were followed to quantify moisture, ash, and volatile of mixed raw powder and produced biochar, respectively. Fixed carbon content (FCC) was computed from 100 % by subtracting these three values [38].

2.3.4. FTIR and SEM analyses

The functional groups of the biochar adsorbent were identified using FTIR (DW-FTIR-530A, China). The biochar samples were combined with KBr in a 1:100 ratios, ground with a mortar, and formed into pellets using a hydraulic pellet press. The analysis was conducted at a resolution of 4 cm^{-1} over a wavenumber range of 400–4000 cm^{-1} [40,41]. The morphological characteristics of the biochar adsorbent were examined using SEM combined with Energy Dispersive X-ray analysis (EDX). It was conducted according to standard SEM operating procedures using a CX-200 instrument from Korea. The SEM was set to operate at an accelerating voltage of 20 kV with a working distance of 16 mm, a magnification of 100×, and a scale of 100 μm, all under high vacuum conditions [42].

2.4. Batch adsorption tests

To conduct batch adsorption tests, a stock solution with a concentration of 1000 mg/L of Cr(VI) was prepared using 2.83 g of $K_2Cr_2O_7$ in 1 L of DW. Calibration standards were prepared based on this stock solution. Table 1 shows ranges of different four parameters taken from the previous studies and used as preliminary tests to examine their effects. The effects of each parameter were studied while keeping others constant. Batch tests were performed based on the previously reported work [33]. The Cr(VI) absorbance in both the test samples and the working standards were measured using AAS at a wavelength of 357.9 nm. The equilibrium concentration of Cr(VI) was determined based on the established calibration curve. Blank solvents were run in between each analysis to correct all absorbance reading measurements for calibration standards and samples. Each batch test was investigated in triplicate, and the final result was reported using averaged mean values with a standard error. Eqs. (2) and (3) were used for determining the efficiency of Cr(VI) adsorption and Cr(VI) adsorbed per unit of biochar adsorbent, respectively [43].

$$\text{Adsorption}\ (\%) = \left(\frac{C_i - C_e}{C_i}\right) \times 100 \tag{2}$$

$$\text{Adsorption capacity}\ (q_e(\text{mg}/\text{g})) = \left(\frac{C_i - C_e}{W_{AC}}\right) \times V \tag{3}$$

Where, C_i and C_e represent the initial and equilibrium concentrations of Cr(VI) (mg/L), respectively. V and W_{AC} denote the total volume (L) and mass of adsorbent (g), respectively.

2.5. Adsorption isotherms

In this work, the interaction mechanism between biochar adsorbent and metal solutions were assessed by utilizing Freundlich and Langmuir's adsorption isotherm models [51]. According to the Langmuir isotherm, the biochar adsorbent's surface contains uniform sites for monolayer adsorption [52,53]. On the other hand, the Freundlich isotherm indicates a multilayer adsorption process and reversible behavior on heterogeneous surfaces [52]. It describes the exponential distribution and variability in surface activity sites of the biochar adsorbent. The linear form of the Langmuir isotherm equation is given by Eq. (4), whereas, the efficiency of the adsorption process, which is determined from the dimensionless Langmuir separation factor (LSF) is shown in Eq. (5) [47]. Eq. (6) was employed to express the linear form of Freundlich adsorption isotherm model [54].

$$\frac{C_e}{q_e} = \frac{1}{q_m \times K_L} + \frac{C_e}{q_m} \tag{4}$$

$$\text{LSF} = \frac{1}{1 + K_L \times C_i} \tag{5}$$

$$\ln(q_e) = \ln(K_f) + {}^{1}/_{n} \ln(C_e) \tag{6}$$

Where, K_L is Langmuir isotherm constant (L/mg), q_m is maximum Langmuir capacity (mg/g), n is Freundlich isotherm adsorption intensity, and K_f is Freundlich isotherm constant (mg/g)/(mg/L)$^{1/n}$.

2.6. Adsorbent reusability and Cr(VI) remediation

Reusability of selected biochar was investigated using the adsorption and desorption processes following the work published elsewhere [55]. The analysis was performed using the optimal parameter values determined from the preliminary test, and 0.1 M NaOH was employed as the eluting agent for the adsorption and desorption cycles. The Cr(VI) desorption test was conducted in 250 mL flask with a known Cr(VI) loaded adsorbent and 100 mL desorption solution of 100 mL was agitated at 200 rpm. In addition, the adsorbent loaded with Cr(VI) was rinsed with DW before drying in an oven at 105 °C for 2 h. The recycled biochar adsorbent was reused for up to four cycles. Eq. (7) was applied to determine the desorption percentage [56].

$$\text{Desorption}\ (\%) = \left(\frac{C_{e(de)}}{C_{e(ads)}}\right) \times 100 \tag{7}$$

Table 1
Different values of parameters from the literature for preliminary batch adsorption tests.

Parameters studied	Selected Values	References
Initial concentration of Cr(VI) (mg/L)	20,30, 50, 70, 90, and 100	[43,44,45]
Contact time (min)	15, 35, 55, 75, and 95	[46]
Solution pH	2, 4, 6, 8, and10	[47,48,45]
Adsorbent dosage (g)	0.1, 0.4, 0.7, 1, and 1.3	[49,50]

Where, $C_{e(de)}$, and $C_{e(ads)}$ (mg/L) denote concentrations of desorbed from biochar adsorbent, and adsorbed on biochar adsorbent at equilibrium, respectively.

3. Results and discussions

3.1. Physicochemical analyses of the synthesized adsorbent

3.1.1. BET surface area analysis

The effect of chemical impregnation on the precursor powder to $ZnCl_2$ ratio on specific surface area (sBET) was investigated (Fig. 3). An increase in impregnation ratio from (1:2) to (1:1) increased the sBET of the adsorbent. Two distinct areas of pore development were observed in Fig. 3. Below the (1:1) ratio, sBET increased significantly from 4.159 to 432.149 m^2/g, while above (1:1), porosity gradually decreased to 285.188 m^2/g at a ratio of 2:1. The formation of multiplayer activators requires a comprehensive understanding of impregnation and carbonization processes [57]. Initially, when corn cob and banana peel biochar are impregnated with $ZnCl_2$, the salt dissociates into Zn^{2+} ions and chloride ions. These Zn^{2+} ions act as catalysts during carbonization, promoting the dehydration and carbonization of organic precursors present in the biomass. In addition, Zn^{2+} ions can promote chemical reactions that heighten the activation of surface functional groups, leading to an increase in the pore volume and surface area of the resulting biochar composite. This phenomenon becomes more evident at higher chemical ratios. Secondly, regarding the role of $ZnCl_2$ in pore development, its impact on the physicochemical properties of biochar composites must be considered. Zn^{2+} ions facilitate the removal of volatile components and enhance the formation of macropores, micropores, and mesopores within the biochar structure [58]. Moreover, $ZnCl_2$ can interact with surface functional groups on the biochar, creating new active sites and altering pore size distribution. A gradual change in the surface porosity of the biochar adsorbent was observed, aligning with previous studies on Cr(VI) removal using activated *Terminalia arjuna nuts* [59].

The carbonization temperature ranges of 500–700 °C was selected based on precursor material thermal degradation characteristics and desired final biochar properties. Higher temperatures generally lead to greater carbonization and graphitization, increasing pore volume and surface area. However, excessively high temperatures could lead to the deterioration of functional groups and a reduction in adsorption capacity. Therefore, the chosen temperature range ensures sufficient carbonization while preserving biochar structure integrity and optimal adsorption properties. Carbonization at 500 °C initially produced insignificant sBET due to insufficient heat for volatile matter evolution and possible inadequate $ZnCl_2$ activation at low temperatures (Fig. 3). As temperatures increased from 500 to 600 °C, more volatiles were released, new pores developed, and sBET increased. Further temperature increments beyond 700 °C led to reduced sBET, attributed to evaporation and contraction of biochar active sites, reducing porosity. Carbonization temperature significantly influences biochar adsorbent properties, with higher temperatures enhancing carbon content, surface area, and adsorption capacity. However, excessively high temperatures can cause pore collapse and decreased efficiency, as reported previously [60–62].

Impregnation times of 60–180 min was chosen to ensure sufficient contact between precursor material and activating agent. Longer impregnation times may result in over-activation, while shorter times may lead to reduced specific surface area as shown in Fig. 3. The selected impregnation time range balances activation efficiency and surface modification avoidance. As impregnation time increased from 60 to 120 min, sBET increased, reaching a local maximum at 120 min before decreasing. Longer carbonation times are desirable to increase biochar porosity, but excessive times can lead to pore closure due to sintering and destroy biochar structure. The choice of impregnation time is crucial, affecting activation and adsorption porosity. Understanding this rationale helps optimize parameters for specific surface areas, as observed in previous work on Cr(VI) adsorption [63,64].

3.1.2. Selection of synthesized biochar adsorbent

In this study, among the synthesized biochar adsorbents (i.e., BP–CCAC@ZC1, BP–CCAC@ZC2, and BP–CCAC@ZC3),

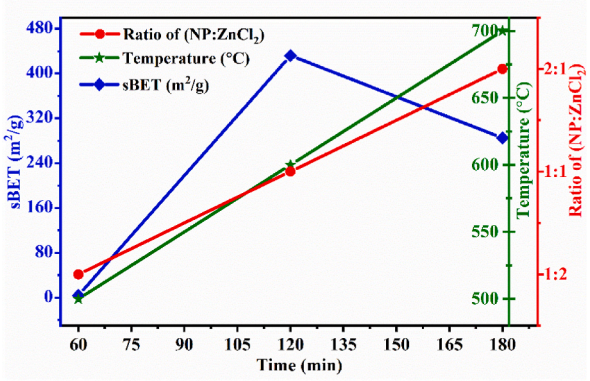

Fig. 3. Effect of the ratio of impregnation, carbonization time, and temperature on sBET.

BP–CCAC@ZC3 was selected as the optimal adsorbent based on its higher sBET (432.149 m^2/g) compared to the other two (4.159 m^2/g and 285.188 m^2/g, respectively) (Table 2). The significantly higher sBET of BP–CCAC@ZC3 compared to BP–CCAC@ZC1 suggests a more extensive network of pores and active sites available for adsorption. This enhanced porosity allows BP–CCAC@ZC3 to accommodate a greater number of chromium ions, thereby enhancing its adsorption performance. Similarly, the superior surface area of BP–CCAC@ZC3 in comparison to BP –CCAC@ZC2 indicates a more optimized pore structure conducive to efficient adsorption. The optimized pore structure of BP–CCAC@ZC3 likely facilitates better contact to active sites and improves the interaction between the adsorbent and chromium ions, resulting in improved adsorption performance. Based on these considerations, further analyses were conducted using the BP–CCAC@ZC3 biochar adsorbent.

3.1.3. Point of zero charge analysis

The success of adsorption processes depends not only on the surface area available on the adsorbent material, but also on the intricate interplay between the adsorbent's surface texture and its inherent electrical properties [36,65]. At a given pH, pHzc specifies the charges on the biochar adsorbent that indicate the potential electrostatics among the adsorbate and adsorbent surfaces. As depicted in Fig. 4, the pHzc value of the BP–CCAC@ZC3 biochar adsorbent in this work was found to be 4.723. Hashem et al. [66] showed that pH values above and below pHzc lead to negatively and positively charged solid surfaces, respectively. The surface of BP–CCAC@ZC3 biochar was positively charged under pH 4.723, and thus its surface adsorbs negatively charged chromate ($HCrO4^-$). The pH-dependent nature of these electrostatic interactions suggests that optimal adsorption occurs under acidic conditions, as the biochar surface becomes positively charged, facilitating the uptake of Cr(VI) ions [67]. Conversely, at pH values above the pHzc, the deprotonation of surface functional groups creates a negatively charged biochar adsorbent surface, repelling negatively charged Cr(VI) ions and thereby reducing adsorption capacity [33]. Generally, the chromium chemical species in aqueous solution, as described by M. M. Islam et al. [68] and Sharma et al. [69], shows the distribution of major Cr^{6+} forms, including $Cr_2O_7^{2-}$, CrO_4^{2-}, H_2CrO_4, and $HCrO_4^-$. Specifically, the predominance of $HCrO_4^-$ occurs in acidic conditions (pH 1–6), while CrO_4^{2-} is the dominant species in alkaline solutions with a pH higher than 7. At a pH < 3.9, Cr^{3+} exists as water-soluble cations, gradually decreasing as pH increases to 5. Hydrolysis causes the formation of $Cr(OH)^{2+}$ at a pH > 5, and insoluble $Cr(OH)_3$ precipitates are formed at a pH > 6 [68].

3.1.4. Proximate analyses of the adsorbents

Table 3 presents the proximate analyses of raw BP–CCP and modified BP–CCAC@ZC3 from this study, along with a comparison to other biochar adsorbents reported in the literature. It can be seen that BP–CCP has a higher volatile (39.6 %), low moisture (11.2 %), high ash content (23.4 %), and high fixed carbon (25.8 %) content. However, BP–CCP activated with $ZnCl_2$ (BP–CCAC@ZC3) resulted in increased fixed carbon content, decreased moisture and ash contents. The BP–CCAC@ZC3 biochar had a moisture content of 2.37 ± 0.80 %. As at higher moisture contents, microorganisms might decompose the biochar surfaces and reduce its adsorption performances, low moisture content of activated carbon is preferable [27]. The modified BP–CCAC@ZC3 also contained 8.07 ± 0.75 % ash and 19.38 ± 2.66 % volatile matter. The occurrence of excessive ash content can cause the pore sites on the biochar adsorbent to become clogged, thereby reducing the adsorption of the adsorbent surface. The research conducted by Bayisa et al. [70] found that an effective means of treating sludge wastewater through adsorption processes is the use of substances with low ash content and medium volatile content, as they indicate greater efficiency. Conversely, adsorbents that have increased proportions of ash and volatiles matter show reduced effectiveness in removing contaminants. The fixed carbon content in biochar activated carbon in the present study was 70.18 %. As shown in Table 3, overall the proximate results of BP–CCAC@ZC3 were in corroborate with the results of previous studies. The removal of ash, moisture, and volatile matter during modification could increase the content of fixed carbon, the formation of porous surfaces, and the graphitization of the produced biochar [71]. High fixed carbon describes high quality and shows better removal efficiency [72]. Based on these findings, the BP–CCAC@ZC3 biochar activated carbon produced from corn cob and banana peel composite activated by $ZnCl_2$ possesses a higher number of carbons–based components, thus demonstrating promising properties as an effective biochar adsorbent.

3.1.5. FTIR analysis

The FTIR spectra of the BP–CCAC@ZC3 adsorbent before and after the adsorption process is depicted in Fig. 5. The peaks observed between 3650 and 3200 cm^{-1} likely correspond to stretching vibrations of amine (N–H) and hydroxyl (O–H) groups, and possibly also to hydrogen bonding between hydroxyl groups [77]. Specifically, the peak at 3436 cm^{-1} indicates the O–H of alcohols and phenols, as well as the N–H vibration of amino acids. The peak band at 2982 cm^{-1} confirms the presence of C–H bonds [47]. Additionally, peaks between 2500 and 2000 cm^{-1} predominantly represent stretching of C⩵C and/or C⩵N bonds [78]. A peak at 2360 cm^{-1} suggests the presence of either cyanide (C⩵N) or alkyne (C⩵C) bending vibrations, while the peak at 1641 cm^{-1} indicates the presence of conjugated systems like alkenes (C═C) or aromatic rings. The band at 1046 cm^{-1} is consistent with C–C or C–O stretching vibrations, potentially indicative of ethers or esters [79]. Likewise, the peak at 580 cm^{-1} can be attributed to vibrations involving Zn–O bonds,

Table 2
Individual outcomes for producing best biochar adsorbent using $ZnCl_2$ activating agent.

Adsorbent code	Temperature (°C)	Time(min)	NP(g)	$ZnCl_2$(g)	(NP: $ZnCl_2$)	sBET (m^2/g)
BP–CCAC@ZC1	500	60	20	40	1:2	4.159
BP–CCAC@ZC2	700	180	40	20	2:1	285.188
BP–CCAC@ZC3	600	120	40	40	1:1	432.149

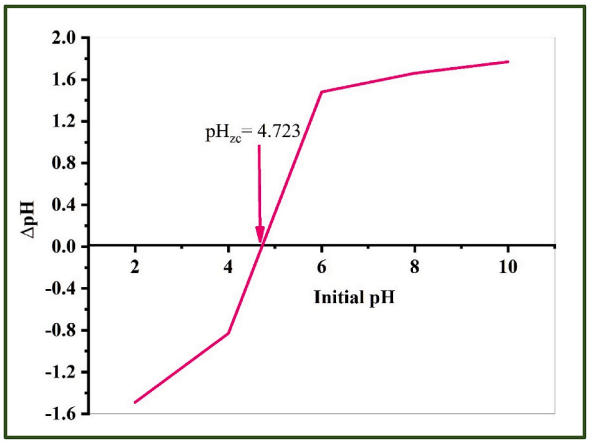

Fig. 4. Plot of point of zero charge.

Table 3
The proximate analysis values of the current biochar and related adsorbents from the literature.

Adsorbent type	Moisture Content (%)	Ash Content (%)	Volatile Matter (%)	FCC (%)	References
Fe_3O_4– Parthenium hysterophorus	5.2	13.3	19.4	62.1	[73]
Corn Cob AC	2.9	2.4	40.9	59.3	[72]
Khat stem AC	6	17.35	20.12	56.53	[70]
Lagerstroemia speciosa Seed hull	3.7	2.6	74.1	19.6	[74]
Bamboo waste AC	9.56	21.66	4.66	73.68	[75]
Coffee husk AC	10.85	3.51	68.33	17.31	[76]
BP–CCP	11.2	23.4	39.6	25.8	This study
BP–CCAC@ZC3 AC	2.37 ± 0.80	8.07 ± 0.75	19.38 ± 2.66	70.18	This study

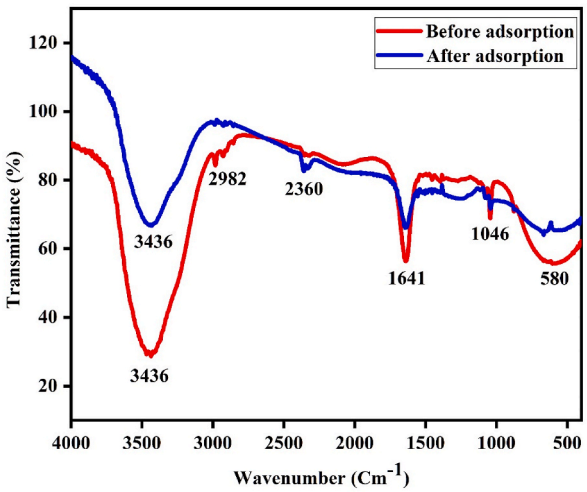

Fig. 5. FTIR analysis of biochar activated carbon before, and after adsorption tests.

potentially serving as a fingerprint for this specific biochar material due to the presence of zinc-containing functional groups [80]. Moreover, the changes in band positions and intensities observed after the adsorption processes can be attributed to the complex interactions and strong binding of surface functional groups with the adsorbate on the biochar surfaces. As the adsorbent interacts with the adsorbate (in this case, Cr(VI)), various chemical reactions occur at the molecular level, leading to alterations in the vibrational frequencies of the functional groups present on the biochar surface. Changes in peak intensities after adsorption signal interactions between the adsorbent and adsorbate molecules. These interactions can involve the formation of new chemical species or the strengthening of existing functional groups on the adsorbent's surface, as seen with hydrogen bonding between the adsorbent and Cr (VI) ions [81]. The study highlights that multifunctional groups on the adsorbent's surface form hydrogen bonds with negatively

charged ($HCrO_4^-$) anions, underscoring the importance of functional groups in facilitating the adsorption process and enhancing the removal of Cr(VI) ions from aqueous solutions.

3.1.6. SEM analysis

Surface morphology analysis was conducted on three samples: the unmodified raw material, the modified activated biochar, and the biochar after Cr(VI) adsorption, as depicted in Fig. 6. The photomicrograph of the unmodified powder (Fig. 6a) showed a rough surface morphology that was tightly packed with no visible open pore surface. This was attributed to the presence of lignin, viscous compounds, and pectin, which could affects adsorption performance [82]. In contrast, the modified adsorbent (Fig. 6b) exhibited open micropores, indicating surface modification through chemical activation by $ZnCl_2$. The evaporation of $ZnCl_2$ and the decomposition of water and other organic substances during carbonization enhanced the biochar's surface area and facilitated the formation of multifunctional groups, as confirmed by FTIR analysis, thus improving adsorption processes. Conversely, Fig. 6c demonstrates a decrease in active surface sites on the biochar following chromium adsorption, implying that the pores have become saturated with Cr (VI) ions. Moreover, The SEM-EDX spectra (Fig. 6d) revealed the presence of a prominent chromium complex peak on the biochar surface, corroborating the study of Fang et al. [83] that observed Cr(VI) occupying biochar pores, thereby diminishing the surface area available for adsorption.

3.2. Effect of parameters on Cr(VI) adsorption

Fig. 7 illustrates the effects of each selected operating parameter on batch Cr(VI) adsorption by BP–CCAC@ZC3 adsorbent. pH values from pH 2 to pH 10 were investigated for Cr(VI) removal while fixing other parameters at average values. The effectiveness of Cr (VI) removal significantly declined from 96.17 %–28.35 % as the pH increased from 2 to 10, as shown in Fig. 7a. A study by Akiode et al. [84] found that the speciation of chromium changes with the pH of the solution. At pH levels higher than 6, chromium ions are present as CrO_4^{2-}. Below pH 1, it exists as $H_2CrO_4^-$, while within pH ranges of 2–6, it exists as $HCrO_4^-$ and $Cr_2O_7^{2-}$ [85]. Therefore, chromium removal was higher under acidic conditions (pH < 6) [86]. The maximum efficiency at lower pH was mainly associated with the positively charged and protonated biochar surface, as confirmed by the *pHzc* study of BP–CCAC@ZC3. The same finding was also noted in the study of [26]. Hence, the maximum adsorption efficiency of BP–CCAC@ZC3 adsorbent was observed at about pH 2. Fig. 7b depicts the efficiency of Cr(VI) adsorption decreased significantly from 90.83 to 54.33 % as the initial concentration of Cr(VI) varied from 20 mg/L to 100 mg/L. The decrements in removal efficiency could be the reason of filling the empty of vacant spaces on adsorbent's surfaces and its saturation with a higher concentration of chromium ions [43]. Badessa et al. [87] reported the same trends in

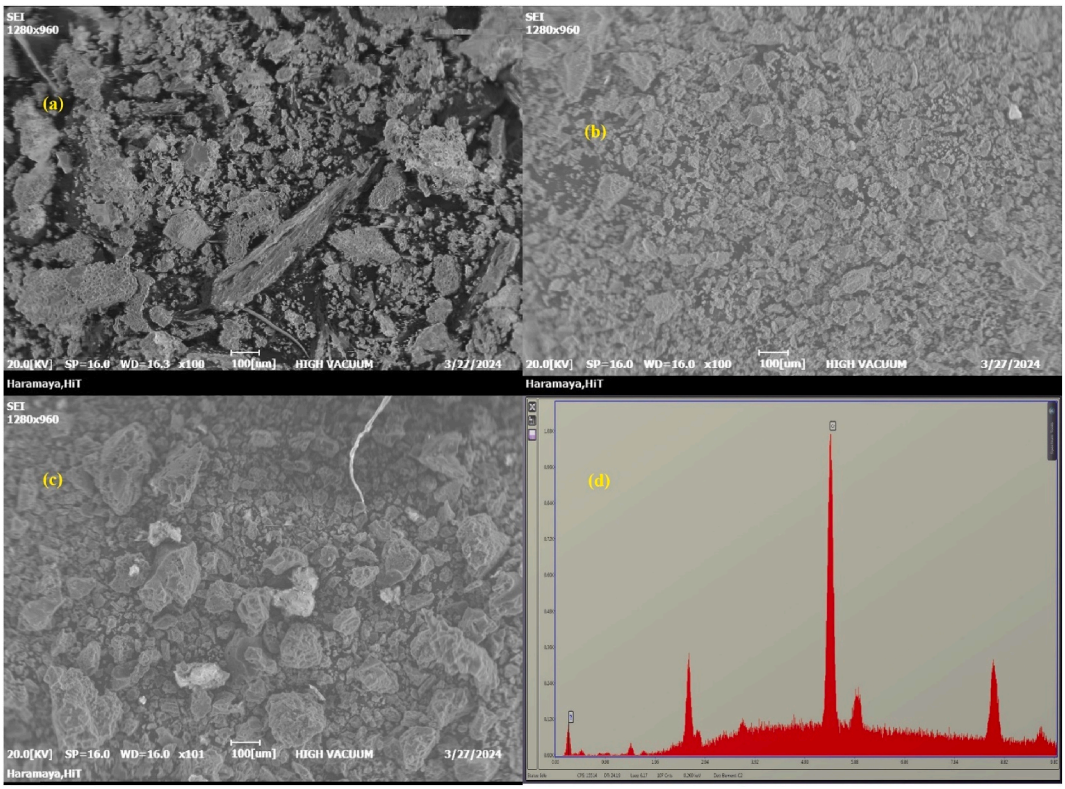

Fig. 6. SEM image analysis of **a** raw sample, **b** modified biochar, **c** after adsorption and **d** EDX after adsorption.

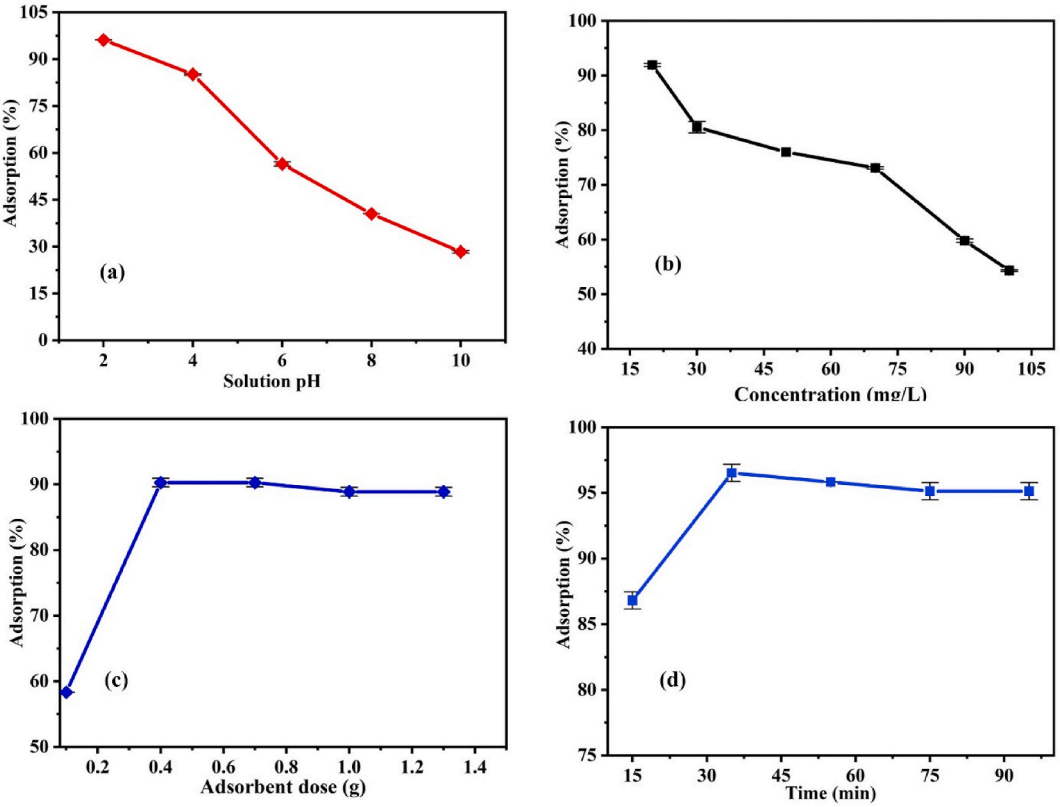

Fig. 7. a Effect of pH (biochar 0.7 g, time 55 min, initial Cr(VI) 50 mg/L), **b** Effect of Cr(VI) concentration (pH 2, time 55 min, biochar 0.7 g), **c** Effect of adsorbent dose (pH 2, biochar 0.4 g, time 55 min), and **d** Effect of time (Cr(VI) 20 mg/L, biochar dose 0.4 g, pH 2).

their study for treating Cr(VI) from sewage wastewater by *banana peel* and *Moringa stenopetala seed* powder. The optimum initial concentration of Cr(VI) (i.e., 20 mg/L) was selected for subsequent adsorption experiments.

Moreover, Fig. 7c reveals effect of BP–CCAC@ZC3 biochar from the ranges of 0.1–1.3 g. Increasing the biochar dose from 0.1 to 0.4 g enhanced adsorption efficiency from 58.33 to 90.28 %, respectively. This adsorption enhancement was possibly due to as the number of adsorbent doses increases; the binding sites available for adsorbing the chromium ion would increase. Nevertheless, increasing the adsorbent dose beyond 0.4 g did not significantly enhance Cr(VI) adsorption efficiency, likely due to an equilibrium reached between the biochar adsorbent and Cr(VI) ions. This finding is concisely consistent to the work that reported treating of heavy metals by banana peel powder [88]. Hence, in this study a biochar dose of 0.4 g was selected as optimal value.

Fig. 7d illustrates the effect of time (varying from 15 to 95 min) on removing Cr(VI) from synthetic aqueous solution. As time enhanced from 15 to 35 min, the Cr(VI) efficiency improved from 86.81 to 96.53 %, respectively. The long interaction time of Cr(VI) ions and the biochar adsorbent's surface contributed to improved adsorption [89]. Though, after reaching equilibria at a time of 35 min, the removal became almost constant, which was due to biochar adsorbent's surface becoming saturated with excess Cr(VI) ions. This finding was corroborated by previous reports [87]. Thus, 35 min was selected as the optimum contact time for Cr(VI) batch tests by BP–CCAC@ZC3. Moreover, numerous studies have been conducted to investigate the effectiveness of different adsorbents for removing Cr(VI) from wastewater. Kumar et al. [90] examined the use of rice straw activated carbon and found that increasing the pH from 3.1 to 8.0 increased Cr(VI) adsorption from 42 %–90 %. However, increasing the concentration of Cr(VI) from 1.5 to 5.0 mg/L decreased adsorption from 74.2 %–47.2 %. Rai et al. [48] also investigated mango kernels activated with H_3PO_4 and achieved an adsorption efficiency of 85 %. Maheshwari & Gupta [91]. utilized fresh non-porous neem bark treated with concentrated H_2SO_4 and obtained a maximum adsorption capacity of 14.33 mg/g. Rangabhashiyam et al. [92] studied *ficus auriculata* leaves and reported a maximum monolayer capacity of 13.33 mg/g of Cr(VI). Badessa et al. [87] examined *Moringa stenopetala* seed powder and banana peel powder, achieving removal efficiencies of 92.17 % and 90.07 %, respectively. Compared to these literatures, this study showed that the mixed composite material had a higher removal efficiency. It achieved a removal efficiency of 97.92 % with a dose of 0.4 g, pH 2, initial concentration of 20 mg/L, and a contact time of 35 min. This indicates that the developed adsorbent performs well and has the potential for efficient removal of Cr(VI) from water/wastewater systems.

3.3. Investigation of adsorption isotherms

In this work, experiments investigated the effect of initial Cr(VI) concentration on its adsorption using isotherms. Analysis of the

linear relationship between C_e and C_e/q_e (as shown in Eq. (4) and Fig. 8a) yielded Langmuir isotherm parameters. The maximum Langmuir adsorption capacity was found to be 19.16 mg/g, signifying that each gram of biochar could adsorb up to this amount within 35 min (Table 4). This result is consistent with similar findings presented in Table 5, highlighting the exceptional capacity of $ZnCl_2$-modified corn cob and banana peel biochar for Cr(VI) removal. On the other hand, the Langmuir model exhibited a superior fit ($R^2 = 0.9977$) compared to the Freundlich model ($R^2 = 0.9726$) (Fig. 8a and b). This suggests a uniform biochar surface and monolayer Cr (VI) adsorption, similar to prior research using sugar beet-based activated carbon [49]. Furthermore, the decreasing LSF values towards zero with increasing initial Cr(VI) concentration (20–70 mg/L) (Fig. 8c) indicate highly favorable Cr(VI) uptake by the BP-CCAC@ZC3 biochar. This effectiveness aligns with studies by Khalifa et al. [93] who employed banana peel-based biochar for Cr (VI) removal in synthetic solutions.

3.4. Adsorbent reusability and remediation studies

Experiments were performed to assess the reusability of the BP-CCAC@ZC3 biochar for Cr(VI) removal from wastewater. Fig. 9 illustrates four consecutive adsorption-desorption cycles conducted under optimal conditions using a 0.1 M NaOH solution. The first cycle achieved an impressive chromium removal efficiency of 97.59 ± 0.57 %, likely due to the abundance of active sites on the biochar surface readily attracting chromium ions (Fig. 9). Additionally, surface functional groups on the biochar may have been protonated, enhancing electrostatic interactions with positively charged chromium species and promoting adsorption. However, a gradual decrease in removal efficiency was observed in subsequent cycles (95.17 ± 0.57, 90.35 ± 1.14 and 84.92 ± 1.14 %, for cycles 2, 3, and 4, respectively). This decline can be attributed to the saturation of active sites on the biochar surface [98]. During the initial cycle, the biochar exhibits a high affinity for chromium, leading to efficient removal. With repeated adsorption-desorption cycles, these sites become progressively occupied, resulting in a reduced capacity to adsorb chromium in subsequent cycles. Several factors may contribute to this decline. The desorption step using NaOH might not fully recover the original adsorption capacity. Residual chromium species may remain bound to the biochar, limiting the availability of active sites for later cycles [99]. Additionally, repeated cycles could compromise the biochar's structural integrity through physical degradation or pore blockage. Furthermore, contaminants or impurities in the wastewater can affect the adsorption-desorption process. The buildup of organic matter or inorganic compounds on the biochar surface during adsorption can hinder the removal of chromium in subsequent cycles.

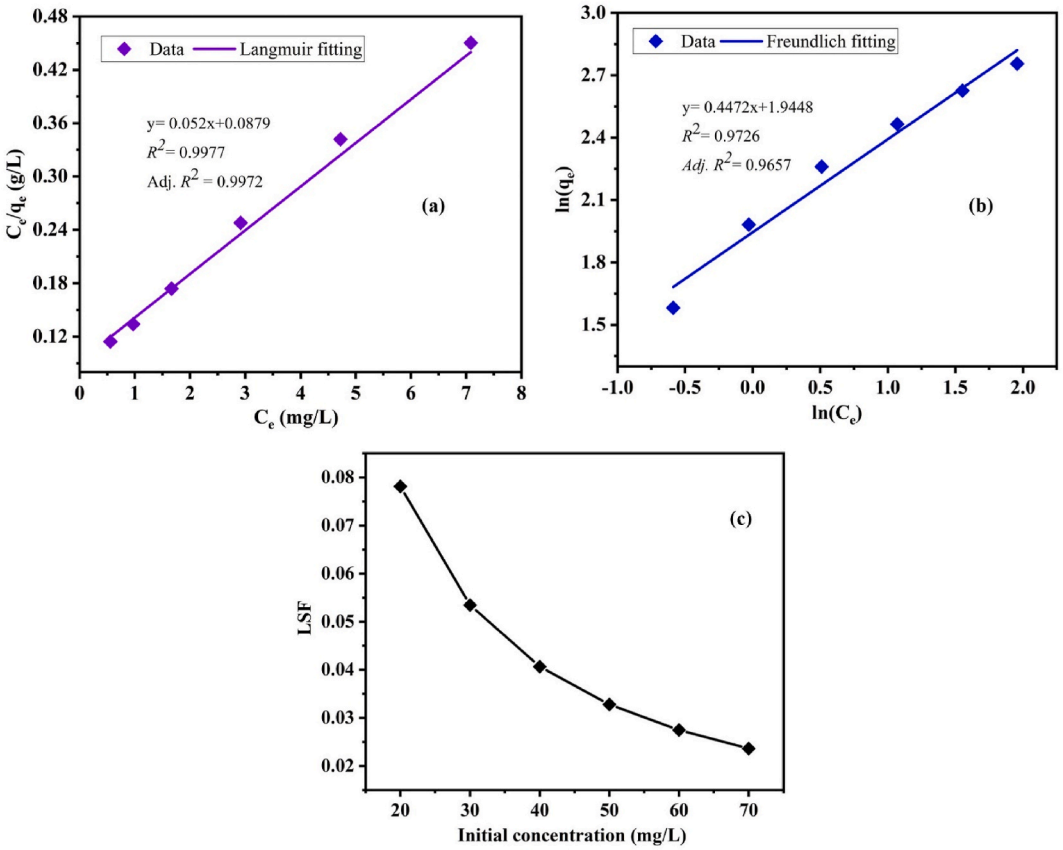

Fig. 8. Model fittings of **a** Langmuir, **b** Freundlich, and **c** LSF versus Cr(VI) initial concentration (at 0.4 g biochar dosage, 35 min contact time, and pH 2).

Table 4
Isotherm parameters values for Langmuir and Freundlich models.

C_i (mg/L)	C_e (mg/L)	q_e (mg/g)	C_e/q_e (g/L)	$\ln(C_e)$	$\ln(q_e)$	Langmuir model				Freundlich model		
						q_m	K_L	LSF	R^2	n	K_f	R^2
20	0.56	4.86	0.11	− 0.59	1.58	19.16	0.59	0.078	0.9977	2.24	6.99	0.9726
30	0.97	7.26	0.13	− 0.03	1.98			0.053				
40	1.67	9.58	0.17	0.51	2.26			0.041				
50	2.92	11.77	0.25	1.07	2.47			0.033				
60	4.72	13.82	0.34	1.55	2.63			0.027				
70	7.08	15.73	0.45	1.96	2.76			0.024				

Table 5
Comparative results of the current study with the corresponding adsorbents in the literature.

Adsorbent types	q_m (mg/g)	Conc. (mg/L)	Dose (g)	Time (min)	pH	References
Teff Straw AC	19.48	87.57	2.742	109	2.2	[42]
MBCAC	98.95 %	23.02	0.354	34.40	2.05	[33]
Corn cob	25.69	50	1	90	2.01	[94]
Arachis hypogea husk	2.355	50	–	120	8.0	[95]
Alga–Fe_3O_4 loaded AC	15.24	40	1	90	3.0	[96]
Mn–Ni Ferrite nanocomposite	18.31	200	0.5	60	9	[35]
Ti–XAD7 nanocomposite	2.73	2.75	5.05	51.53	8.7	[97]
Mango kernel AC	7.8	60	0.25	150	–	[48]
Leucaena leucocephala AC	13.85	100	0.3	60	4	[50]
Parthenium hysterophorus weed	24.9	100	0.9	90	2	[27]
Turbinaria vulgaris	21.8	100	1.2	110	2.8	[86]
BP–CCAC@ZC3 AC	19.16	20	0.4	35	2	**This study**

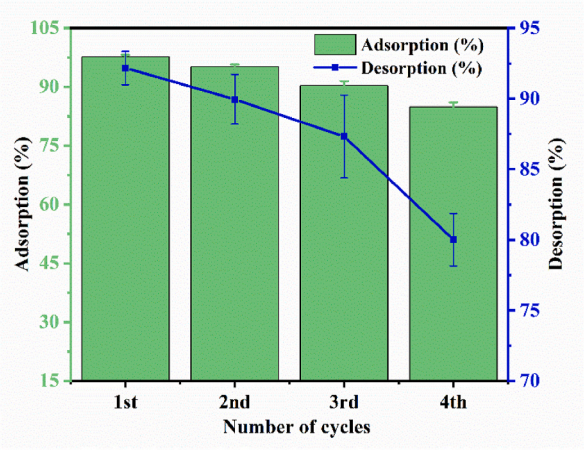

Fig. 9. Desorption and adsorption performances of Cr(VI) removal using recycled and fresh adsorbents.

Despite the observed decrease, the BP-CCAC@ZC3 biochar demonstrates excellent reusability compared to existing adsorbents. Studies by Ashour & Tony [100] and Ma et al. [101] reported significantly lower regeneration efficiencies (59 % and 52.39 %) for clay minerals and corn straw, respectively, after similar cycles. This comparison highlights the superior reusability and regeneration potential of the BP-CCAC@ZC3 biochar for practical applications in Cr(VI) wastewater treatment.

3.5. Possible adsorption mechanisms

Based on the current results of this research study, anionic chromate was easily adsorbed from the surface of biochar adsorbent because of the adsorbent's complex chemical structures, and the abundance of binding sites on BP–CCAC@ZC3. Adsorption mechanisms of Cr(VI) on the biochar surface were realized by complex formation, redox process, and electrostatic interactions. The FTIR spectrum results confirmed that surface functions such as O–H, C–O, N–H, C≡N, C–H, C≡C, C–C, and C═C formed bond complexes with Cr(VI). The reductions of hexavalent to trivalent chromium occurred on the biochar surfaces via the redox processes. The reduction mechanism is presented in Eq. (8) [89]. Comparatively, Cr^{3+} was more easily attracted by electrostatic attraction than other

chromium species on the heterogeneous surfaces of adsorbents. Furthermore, under acidic conditions, the negatively charged anionic chromate ($HCrO4^{-}$) easily binds to the positively charged BP–CCAC@ZC3 adsorbent through electrostatic attraction [66].

$$HCrO_4^- + 7H^+ + 3e^- \leftrightarrow Cr^{3+} + 4H_2O \quad (8)$$

4. Conclusions

This study successfully synthesized a BP-CCAC@ZC3 biochar adsorbent by using a mixture of corn cob and banana peel, with $ZnCl_2$ as the activating agent for reducing Cr(VI) from synthetic solutions. Through preliminary testing, optimal conditions were determined to achieve a high-porosity adsorbent, including an impregnation ratio of NP to $ZnCl_2$ at 1:1 by weight, a carbonization temperature of 600 °C for 2 h, resulting in a specific surface area (sBET) value of approximately 432.149 m^2/g. The sBET results confirmed that BP-CCAC@ZC3 exhibited the highest porosity among the tested biochars, making it effective for mitigating Cr(VI) from synthetic solutions. Physicochemical surface characteristics were evaluated using proximate analyses, surface charge analysis, and SEM, and the results indicated that this biochar was a potential candidate for adsorption applications. The FTIR spectra analysis confirmed the presence of multifunctional groups on the surface of the selected adsorbent, which play a significant role in the removal of Cr(VI). The effects of parameters including pH (2–10), time (15–95 min), biochar dose (0.1–1.3 g), and (20–100 mg/L) of initial Cr(VI) concentration were investigated through batch adsorptions. The maximum 97.92 % of Cr(VI) removal was found at a biochar dosage of 0.4 g, pH 2, an initial Cr(VI) concentration of 20 mg/L and a contact time of 35 min. The data from the experiment showed a strong fit with the Langmuir isotherm model ($R^2 = 0.9977$), suggesting that the adsorption process was uniform and occurred at a monolayer level. The adsorption-desorption cycles demonstrated that BP-CCAC@ZC3 biochar exhibited excellent stability and reusability, maintaining over 80 % adsorption efficiency of Cr(VI) in practical applications for up to four cycles. This underscores the effectiveness of this biochar in remediation of Cr(VI) from synthetic solutions.

In summary, using corn cob and banana peel composites to produce activated carbon provides a sustainable and eco-friendly approach to tackling pollution and waste disposal problems. This approach proves effective for removing Cr(VI) from synthetic solutions, showcasing promise for environmental remediation efforts. Nevertheless, to broaden the applicability of this composite adsorbent, future investigations should assess the adsorbent's efficacy against a wider range of heavy metals prevalent in industrial wastewater, particularly those from tannery operations. Additionally, optimizing process parameters like temperature, agitation speed, and particle size has the potential to significantly enhance adsorption efficiency. Furthermore, a thermodynamic evaluation of the adsorption mechanism would provide valuable insights into the process. Finally, validating the real-world applicability of this adsorbent requires pilot and column-based adsorption experiments that simulate industrial-scale wastewater treatment.

Compliance with ethical standards

The authors declare that ethical considerations were taken into account while writing the manuscript.

Funding

The current work has not received any form of funding from the agencies/organizations.

Data availability

Data will be made available on a reasonable request from the corresponding author.

Ethical clearance and consent to participate

The experimental paper does not involve human subjects.

Consent to publish

We declare that there are no conflicts of interest associated with this manuscript. As the corresponding author, we confirm that the manuscript has been proofread and approved for resubmission by all named authors.

CRediT authorship contribution statement

Hirpha Adugna Areti: Writing – review & editing, Writing – original draft, Visualization, Validation, Software, Methodology, Investigation, Formal analysis, Data curation, Conceptualization. **Abdisa Jabesa:** Writing – review & editing, Writing – original draft, Visualization, Validation, Supervision, Project administration, Methodology, Investigation, Formal analysis, Data curation, Conceptualization. **Melkiyas Diriba Muleta:** Writing – review & editing, Visualization, Supervision, Methodology, Formal analysis. **Abdi Nemera Emana:** Writing – review & editing, Visualization, Supervision, Methodology, Investigation, Formal analysis.

Declaration of competing interest

The authors declare that they have no known competing financial interests or personal relationships that could have appeared to influence the work reported in this paper.

Acknowledgement

The authors gratefully acknowledge the Department of Chemical Engineering at Haramaya Institute of Technology, Haramaya University, for their support and provision of essential laboratory facilities, which were instrumental in completing this research. We would also like to express our sincere appreciation to **Mr. Firomsa Dadi** from the Department of Mechanical Engineering at Haramaya Institute of Technology, Haramaya University, for his invaluable assistance and cooperation during the SEM-EDX analysis.

References

[1] M. Birhanie, S. Leta, M.M. Khan, Treatment of tannery wastewater to remove hazardous pollutants by scoria (volcanic ash) a low cost adsorbent, Int. J. Environ. Agric. Biotechnol. 2 (2017) 2841–2849, https://doi.org/10.22161/ijeab/2.6.10.
[2] M. Zhao, Y. Xu, C. Zhang, H. Rong, G. Zeng, New trends in removing heavy metals from wastewater, Appl. Microbiol. Biotechnol. 100 (2016) 6509–6518, https://doi.org/10.1007/s00253-016-7646-x.
[3] L. Joseph, B.-M. Jun, J.R. V Flora, C.M. Park, Y. Yoon, Removal of heavy metals from water sources in the developing world using low-cost materials: a review, Chemosphere 229 (2019) 142–159, https://doi.org/10.1016/j.chemosphere.2019.04.198.
[4] M. Tumolo, V. Ancona, D. De Paola, D. Losacco, C. Campanale, C. Massarelli, V.F. Uricchio, Chromium pollution in European water, sources, health risk, and remediation strategies: an overview, Int. J. Environ. Res. Publ. Health 17 (2020) 5438, https://doi.org/10.3390/ijerph17155438.
[5] S. Vieto, D. Rojas-Gätjens, J.I. Jiménez, M. Chavarría, The potential of Pseudomonas for bioremediation of oxyanions, Environ. Microbiol. Rep. 13 (2021) 773–789, https://doi.org/10.1111/1758-2229.12999.
[6] O.P. Karthikeyan, T.J. Smith, S.U. Dandare, K.S. Parwin, H. Singh, H.X. Loh, M.R. Cunningham, P.N. Williams, T. Nichol, A. Subramanian, K. Ramasamy, D. Kumaresan, Metal(loid) speciation and transformation by aerobic methanotrophs, Microbiome 9 (2021) 156, https://doi.org/10.1186/s40168-021-01112-y.
[7] R.T. Kapoor, M.R. Salvadori, M. Rafatullah, M.R. Siddiqui, M.A. Khan, S.A. Alshareef, Exploration of microbial factories for synthesis of nanoparticles – a sustainable approach for bioremediation of environmental contaminants, Front. Microbiol. 12 (2021), https://doi.org/10.3389/fmicb.2021.658294.
[8] M. Choudhary, S. Gupta, M.K. Dhar, S. Kaul, Endophytic fungi-mediated biocatalysis and biotransformations paving the way toward green chemistry, Front. Bioeng. Biotechnol. 9 (2021), https://doi.org/10.3389/fbioe.2021.664705.
[9] R.S. Boddu, O. Perumal, D. K, Microbial nitroreductases: a versatile tool for biomedical and environmental applications, Biotechnol. Appl. Biochem. (2020), https://doi.org/10.1002/bab.2073 bab.2073.
[10] P. Karthikeyan, K. Ramkumar, K. Pandi, A. Fayyaz, S. Meenakshi, C.M. Park, Effective removal of Cr(VI) and methyl orange from the aqueous environment using two-dimensional (2D) Ti3C2Tx MXene nanosheets, Ceram. Int. 47 (2021) 3692–3698, https://doi.org/10.1016/j.ceramint.2020.09.221.
[11] R. Wang, Y. Li, X. Shuai, J. Chen, R. Liang, C. Liu, Development of pectin-based aerogels with several excellent properties for the adsorption of Pb2+, Foods 10 (2021) 3127, https://doi.org/10.3390/foods10123127.
[12] L. Li, Y. Xie, K. Chen, J. Zhou, M. Wang, W. Wang, Z. Zhang, F. Lu, Y. Du, Y. Feng, Adsorption characteristics of ball milling-modified Chinese medicine residue biochar toward quercetin, ACS Omega 9 (2024) 11658–11670, https://doi.org/10.1021/acsomega.3c09016.
[13] Y. Liu, R. Pei, Y. Lv, C. Lin, J. Huang, M. Liu, Removal behavior and mechanism of silver from low concentration wastewater using cellulose aerogel modified by thiosemicarbazide, J. Appl. Polym. Sci. 138 (2021), https://doi.org/10.1002/app.51226.
[14] H. Peng, J. Guo, Removal of chromium from wastewater by membrane filtration, chemical precipitation, ion exchange, adsorption electrocoagulation, electrochemical reduction, electrodialysis, electrodeionization, photocatalysis and nanotechnology: a review, Environ. Chem. Lett. 18 (2020) 2055–2068, https://doi.org/10.1007/s10311-020-01058-x.
[15] M.Z.A. Zaimee, M.S. Sarjadi, M.L. Rahman, Heavy metals removal from water by efficient adsorbents, Water 13 (2021) 2659, https://doi.org/10.3390/w13192659.
[16] A. Arami-Niya, T.E. Rufford, Z. Zhu, Nitrogen-Doped carbon foams synthesized from banana peel and zinc complex template for adsorption of CO 2 , CH 4 , and N 2, Energy & Fuels 30 (2016) 7298–7309, https://doi.org/10.1021/acs.energyfuels.6b00971.
[17] A.K. Tolkou, K.N. Maroulas, D. Theologis, I.A. Katsoyiannis, G.Z. Kyzas, Comparison of Modified Peels: Natural Peels or Peels-Based Activated Carbons for the Removal of Several Pollutants Found in Wastewaters 10 (2024) 22, https://doi.org/10.3390/c10010022. C.
[18] P.D. Pathak, S.A. Mandavgane, B.D. Kulkarni, Fruit peel waste as a novel low-cost bio adsorbent, Rev. Chem. Eng. 31 (2015), https://doi.org/10.1515/revce-2014-0041.
[19] S. De Gisi, G. Lofrano, M. Grassi, M. Notarnicola, Characteristics and adsorption capacities of low-cost sorbents for wastewater treatment: a review, Sustain. Mater. Technol. 9 (2016) 10–40, https://doi.org/10.1016/j.susmat.2016.06.002.
[20] N. Abd-Talib, C.S. Chuong, S.H. Mohd-Setapar, U.A. Asli, K.F. Pa'ee, K.Y.T. Len, Trends in adsorption mechanisms of fruit peel adsorbents to remove wastewater pollutants (Cu (II), Cd (II) and Pb (II)), J. Water Environ. Technol. 18 (2020) 290–313, https://doi.org/10.2965/jwet.20-004.
[21] S. Martini, D. KharismadewiMardwita, Y.R. Ginting, Biomass potential as an alternative resource for valuable products in the perspective of environmental sustainability and a circular economy system, IOP Conf. Ser. Earth Environ. Sci. 1175 (2023) 012012, https://doi.org/10.1088/1755-1315/1175/1/012012.
[22] S. Bose, A. Ghosh, A. Das, M. Rahaman, Development of mango peel derived activated carbon-nickel nanocomposite as an adsorbent towards removal of heavy metal and organic dye removal from aqueous solution, ChemistrySelect 5 (2020) 14168–14176, https://doi.org/10.1002/slct.202003606.
[23] A. Rahmayanti, A. Firdaus, M. Tamyiz, L.N. Hamidah, L. Oktavia, E. Rosyidah, A. Widiyanti, Synthesis and effectiveness of snake fruit (salacca zalacca) seed charcoal bio-adsorbent in reducing remazol brilliant blue, IOP Conf. Ser. Earth Environ. Sci. 1030 (2022) 012016, https://doi.org/10.1088/1755-1315/1030/1/012016.
[24] K. Mahalakshmi Sangeetha, P. Kavya, Formulation and quality evaluation of fruit peel powder incorporated cookies, FoodSci Indian J. Res. Food Sci. Nutr. 6 (2019) 16, https://doi.org/10.15613/fijrfn/2019/v6i1/184224.
[25] A. Moges, T.T.I. Nkambule, J. Fito, The application of GO-Fe3O4 nanocomposite for chromium adsorption from tannery industry wastewater, J. Environ. Manage. 305 (2022) 114369, https://doi.org/10.1016/j.jenvman.2021.114369.
[26] T. Adane, D. Haile, A. Dessie, Y. Abebe, H. Dagne, Response surface methodology as a statistical tool for optimization of removal of chromium (VI) from aqueous solution by Teff (Eragrostis teff) husk activated carbon, Appl. Water Sci. 10 (2019) 37, https://doi.org/10.1007/s13201-019-1120-8.
[27] D. Bedada, K. Angassa, A. Tiruneh, H. Kloos, J. Fito, Chromium removal from tannery wastewater through activated carbon produced from Parthenium hysterophorus weed, Energy, Ecol. Environ. 5 (2020) 184–195, https://doi.org/10.1007/s40974-020-00160-8.
[28] T.A. Amibo, S.M. Beyan, T.M. Damite, Novel lanthanum doped magnetic teff straw biochar nanocomposite and optimization its efficacy of defluoridation of groundwater using RSM: a case study of Hawassa city, Ethiopia, Adv. Mater. Sci. Eng. 2021 (2021) 1–15, https://doi.org/10.1155/2021/9444577.
[29] S.P. Tripathy, S. Subudhi, A. Ray, P. Behera, A. Bhaumik, K. Parida, Mixed-valence bimetallic Ce/Zr MOF-based nanoarchitecture: a visible-light-active photocatalyst for ciprofloxacin degradation and hydrogen evolution, Langmuir 38 (2022) 1766–1780, https://doi.org/10.1021/acs.langmuir.1c02873.

[30] T.E. Kibona, D.J. Mahushi, G.N. Shao, Highly microporous and mesoporous nanomaterials derived from <scp> *Agave sisalana* </scp> waste for supercapacitors, Biofuels, Bioprod. Biorefining 17 (2023) 1554–1565, https://doi.org/10.1002/bbb.2523.

[31] J. Phuriragpitikhon, K. Pluamjai, W. Fuangchoonuch, L. Chuenchom, Conversion of cassava rhizome into efficient carbonaceous adsorbents for removal of dye in water, IOP Conf. Ser. Earth Environ. Sci. 1139 (2023) 012003, https://doi.org/10.1088/1755-1315/1139/1/012003.

[32] C. Rattanet, J.T.N. Knijnenburg, Y. Ngernyen, Kinetics and isotherm studies of methylene blue adsorption on activated carbon derived from Chrysanthemum: solid waste of beverage industry, J. Japan Inst. Energy 101 (2022) 122–131, https://doi.org/10.3775/jie.101.122.

[33] H.A. Areti, A. Jabesa, B.J. Daba, D. Jibril, Response surface method based parametric optimization of Cr(VI) removal from tannery wastewater using a mixed banana peel and corn cob activated carbon: kinetic and isotherm modeling studies, J. Water Process Eng. 59 (2024) 104977, https://doi.org/10.1016/j.jwpe.2024.104977.

[34] D. Prabu, P.S. Kumar, B.S. Rathi, S. Sathish, K.V. Anand, J.A. Kumar, O.B. Mohammed, P. Silambarasan, Feasibility of magnetic nano adsorbent impregnated with activated carbon from animal bone waste: application for the chromium (VI) removal, Environ. Res. 203 (2022) 111813, https://doi.org/10.1016/j.envres.2021.111813.

[35] J. Fito, O. Ebrahim, T.T.I. Nkambule, The application Mn-Ni ferrite nanocomposite for adsorption of chromium from textile industrial wastewater, Water Air Soil Pollut. 234 (2023) 37, https://doi.org/10.1007/s11270-022-06058-x.

[36] A. Saravanan, P.S. Kumar, S. Varjani, S. Karishma, S. Jeevanantham, P.R. Yaashikaa, Effective removal of Cr (VI) ions from synthetic solution using mixed biomasses: kinetic, equilibrium and thermodynamic study, J. Water Process Eng. 40 (2021) 101905, https://doi.org/10.1016/j.jwpe.2020.101905.

[37] A. Tebeje, Z. Worku, T.T.I. Nkambule, J. Fito, Adsorption of chemical oxygen demand from textile industrial wastewater through locally prepared bentonite adsorbent, Int. J. Environ. Sci. Technol. 19 (2022) 1893–1906, https://doi.org/10.1007/s13762-021-03230-4.

[38] P. González-García, S. Gamboa-González, I. Andrade Martinez, T. Hernández-Quiroz, Preparation of activated carbon from water hyacinth stems by chemical activation with K2CO3 and its performance as adsorbent of sodium naproxen, Environ. Prog. Sustain. Energy 39 (2020) 13366, https://doi.org/10.1002/ep.13366.

[39] J. Fito, S. Tibebu, T.T.I. Nkambule, Optimization of Cr (VI) removal from aqueous solution with activated carbon derived from Eichhornia crassipes under response surface methodology, BMC Chem 17 (2023) 4, https://doi.org/10.1186/s13065-023-00913-6.

[40] Q. Liu, B. Yang, L. Zhang, R. Huang, Adsorptive removal of Cr (VI) from aqueous solutions by cross-linked chitosan/bentonite composite, Kor. J. Chem. Eng. 32 (2015) 1314–1322, https://doi.org/10.1007/s11814-014-0339-1.

[41] J. Fito, S. Tibebu, T.T.I. Nkambule, Optimization of Cr (VI) removal from aqueous solution with activated carbon derived from Eichhornia crassipes under response surface methodology, BMC Chem 17 (2023) 4, https://doi.org/10.1186/s13065-023-00913-6.

[42] S.M. Beyan, S.V. Prabhu, T.A. Ambio, C. Gomadurai, Research Article A Statistical Modeling and Optimization for Cr (VI) Adsorption from Aqueous Media via Teff Straw-Based Activated Carbon : Isotherm , Kinetics , and Thermodynamic Studies, 2022, p. 2022.

[43] R. Giri, N. Kumari, M. Behera, A. Sharma, S. Kumar, N. Kumar, R. Singh, Adsorption of hexavalent chromium from aqueous solution using pomegranate peel as low-cost biosorbent, Environ. Sustain 4 (2021) 401–417, https://doi.org/10.1007/s42398-021-00192-8.

[44] F. Benmahdi, S. Khettaf, M. Kolli, Efficient removal of Cr(VI) from aqueous solution using activated carbon synthesized from silver berry seeds: modeling and optimization using central composite design, Biomass Convers. Biorefinery (2022) 1–15, https://doi.org/10.1007/s13399-022-03041-8.

[45] F.-L. Long, C.-G. Niu, N. Tang, H. Guo, Z.-W. Li, Y.-Y. Yang, L.-S. Lin, Highly efficient removal of hexavalent chromium from aqueous solution by calcined Mg/Al-layered double hydroxides/polyaniline composites, Chem. Eng. J. 404 (2021) 127084, https://doi.org/10.1016/j.cej.2020.127084.

[46] V.G. Georgieva, M.P. Tavlieva, S.D. Genieva, L.T. Vlaev, Adsorption kinetics of Cr (VI) ions from aqueous solutions onto black rice husk ash, J. Mol. Liq. 208 (2015) 219–226, https://doi.org/10.1016/j.molliq.2015.04.047.

[47] G.K. Gupta, M.K. Mondal, Mechanism of Cr(VI) uptake onto sagwan sawdust derived biochar and statistical optimization via response surface methodology, Biomass Convers. Biorefinery 13 (2023) 709–725, https://doi.org/10.1007/s13399-020-01082-5.

[48] M.K. Rai, G. Shahi, V. Meena, R. Meena, S. Chakraborty, R.S. Singh, B.N. Rai, Removal of hexavalent chromium Cr (VI) using activated carbon prepared from mango kernel activated with H3PO4, Resour. Technol. 2 (2016) S63–S70, https://doi.org/10.1016/j.reffit.2016.11.011.

[49] F. Ghorbani, S. Kamari, S. Zamani, S. Akbari, M. Salehi, Optimization and modeling of aqueous Cr (VI) adsorption onto activated carbon prepared from sugar beet bagasse agricultural waste by application of response surface methodology, Surface. Interfac. 18 (2020) 100444, https://doi.org/10.1016/j.surfin.2020.100444.

[50] K. Malwade, D. Lataye, V. Mhaisalkar, S. Kurwadkar, D. Ramirez, Adsorption of hexavalent chromium onto activated carbon derived from Leucaena leucocephala waste sawdust: kinetics, equilibrium and thermodynamics, Int. J. Environ. Sci. Technol. 13 (2016) 2107–2116, https://doi.org/10.1007/s13762-016-1042-z.

[51] I. Loulidi, F. Boukhlifi, M. Ouchabi, A. Amar, M. Jabri, A. Kali, C. Hadey, Assessment of untreated coffee wastes for the removal of chromium (VI) from aqueous medium, Int. J. Chem. Eng. 2021 (2021) 9977817, https://doi.org/10.1155/2021/9977817.

[52] H.A. Isiyaka, K. Jumbri, N.S. Sambudi, Z.U. Zango, N. Abdullah, B. Saad, Optimizations and docking simulation study for metolachlor adsorption from water onto MIL-101 (Cr) metal–organic framework, Int. J. Environ. Sci. Technol. 20 (2023) 277–292, https://doi.org/10.1007/s13762-022-04059-1.

[53] D.T. Mekonnen, E. Alemayehu, B. Lennartz, Adsorptive removal of phosphate from aqueous solutions using low-cost volcanic rocks: kinetics and equilibrium approaches, Materials 14 (2021) 1312, https://doi.org/10.3390/ma14051312.

[54] I.U. Islam, M. Ahmad, M. Ahmad, S. Rukh, I. Ullah, Kinetic studies and adsorptive removal of chromium Cr (VI) from contaminated water using green adsorbent prepared from agricultural waste, rice straw, Eur. J. Chem. 13 (2022) 78–90, https://doi.org/10.5155/eurjchem.13.1.78-90.2189.

[55] D.R. Vaddi, T.R. Gurugubelli, R. Koutavarapu, D.-Y. Lee, J. Shim, Bio-stimulated adsorption of Cr (VI) from aqueous solution by groundnut shell activated carbon@ Al embedded material, Catalysts 12 (2022) 290, https://doi.org/10.3390/catal12030290.

[56] J. Bayuo, M. Rwiza, K. Mtei, Response Surface Optimization and Modeling in Heavy Metal Removal from Wastewater—A Critical Review, Springer International Publishing, 2022, https://doi.org/10.1007/s10661-022-09994-7.

[57] A. Fletcher, T. Somorin, O. Aladeokin, Production of high surface area activated carbon from peanut shell by chemical activation with zinc chloride: optimisation and characterization, BioEnergy Res 17 (2023) 467–478, https://doi.org/10.1007/s12155-023-10683-7.

[58] D. An, Y. Sun, Y.-L. Yang, X.-L. Shi, H.-J. Chen, L. Zhang, G. Suo, X. Hou, X. Ye, S. Lu, Z.-G. Chen, A strategy-purifying wastewater with waste materials: Zn2+ modified waste red mud as recoverable adsorbents with an enhanced removal capacity of Congo red, J. Colloid Interface Sci. 645 (2023) 694–704, https://doi.org/10.1016/j.jcis.2023.04.176.

[59] K. Mohanty, M. Jha, B.C. Meikap, M.N. Biswas, Removal of chromium (VI) from dilute aqueous solutions by activated carbon developed from Terminalia arjuna nuts activated with zinc chloride, Chem. Eng. Sci. 60 (2005) 3049–3059, https://doi.org/10.1016/j.ces.2004.12.049.

[60] Ö. Şahin, C. Saka, A.A. Ceyhan, O. Baytar, Preparation of high surface area activated carbon from elaeagnus angustifolia seeds by chemical activation with ZnCl2 in one-step treatment and its iodine adsorption, Separ. Sci. Technol. 50 (2015) 886–891, https://doi.org/10.1080/01496395.2014.966204.

[61] P. Feng, J. Li, H. Wang, Z. Xu, Biomass-based activated carbon and activators: preparation of activated carbon from corncob by chemical activation with biomass pyrolysis liquids, ACS Omega 5 (2020) 24064–24072, https://doi.org/10.1021/acsomega.0c03494.

[62] G. Cruz, M. Pirilä, M. Huuhtanen, L. Carrión, E. Alvarenga, R.L. Keiski, Production of activated carbon from cocoa (Theobroma cacao) pod husk, J. Civ. Environ. Eng. 2 (2012) 1–6, https://doi.org/10.4172/2165-784X.1000109.

[63] A.G.M. Shoaib, A. El-Sikaily, A. El Nemr, A.E.-D.A. Mohamed, A.A. Hassan, Testing the carbonization condition for high surface area preparation of activated carbon following type IV green alga Ulva lactuca, Biomass Convers. Biorefinery 12 (2022) 3303–3318, https://doi.org/10.1007/s13399-020-00823-w.

[64] B.R. Patra, S. Nanda, A.K. Dalai, V. Meda, Taguchi-based process optimization for activation of agro-food waste biochar and performance test for dye adsorption, Chemosphere 285 (2021) 131531, https://doi.org/10.1016/j.chemosphere.2021.131531.

[65] M. Asanu, D. Beyene, A. Befekadu, Removal of hexavalent chromium from aqueous solutions using natural zeolite coated with magnetic nanoparticles: optimization, kinetics, and equilibrium studies, Adsorpt. Sci. Technol. 2022 (2022) 8625489, https://doi.org/10.1155/2022/8625489.

[66] M.A. Hashem, S. Mim, S. Payel, M.Z.R. Shaikh, M.S. Nur-A-Tomal, Comparative chromium adsorption studies on thermally and chemical-thermally modified Ficus carica adsorbents, Int. J. Environ. Sci. Technol. 20 (2023) 12363–12378, https://doi.org/10.1007/s13762-023-04806-y.

[67] D. Xu, T. Sun, H. Jia, Y. Sun, X. Zhu, The performance and mechanism of Cr(VI) adsorption by biochar derived from Potamogeton crispus at different pyrolysis temperatures, J. Anal. Appl. Pyrolysis 167 (2022) 105662, https://doi.org/10.1016/j.jaap.2022.105662.

[68] M.M. Islam, A.A. Mohana, M.A. Rahman, M. Rahman, R. Naidu, M.M. Rahman, A comprehensive review of the current progress of chromium removal methods from aqueous solution, Toxics 11 (2023), https://doi.org/10.3390/toxics11030252.

[69] S.K. Sharma, B. Petrusevski, G. Amy, Chromium removal from water: a review, J. Water Supply Res. Technol. 57 (2008) 541–553, https://doi.org/10.2166/aqua.2008.080.

[70] Y.M. Bayisa, T.A. Bullo, D.A. Akuma, Chromium removal from tannery effluents by adsorption process via activated carbon chat stems (Catha edulis) using response surface methodology, BMC Res. Notes 14 (2021) 431, https://doi.org/10.1186/s13104-021-05855-7.

[71] Z. Ab Ghani, M.S. Yusoff, N.Q. Zaman, M.F.M.A. Zamri, J. Andas, Optimization of preparation conditions for activated carbon from banana pseudo-stem using response surface methodology on removal of color and COD from landfill leachate, Waste Manag. 62 (2017) 177–187, https://doi.org/10.1016/j.wasman.2017.02.026.

[72] T. Sime, J. Fito, T.T.I. Nkambule, Y. Temesgen, A. Sergawie, Adsorption of Congo red from textile wastewater using activated carbon developed from corn cobs : the studies of isotherms and kinetics, Chem. Africa (2023), https://doi.org/10.1007/s42250-022-00583-2.

[73] J. Fito, M. Abewaa, T. Nkambule, Magnetite-impregnated biochar of parthenium hysterophorus for adsorption of Cr(VI) from tannery industrial wastewater, Appl. Water Sci. 13 (2023) 78, https://doi.org/10.1007/s13201-023-01880-y.

[74] A. Nawaz, B. Singh, P. Kumar, H3PO4-modified Lagerstroemia speciosa seed hull biochar for toxic Cr(VI) removal: isotherm, kinetics, and thermodynamic study, Biomass Convers. Biorefinery 13 (2023) 7027–7041, https://doi.org/10.1007/s13399-021-01780-8.

[75] T. Dula, K. Siraj, S.A. Kitte, Adsorption of hexavalent chromium from aqueous solution using chemically activated carbon prepared from locally available waste of bamboo (oxytenanthera abyssinica), ISRN Environ. Chem. 2014 (2014) 438245, https://doi.org/10.1155/2014/438245.

[76] A.T. Abeto, S.M. Beyan, B.A. Bekele, K.W. Firomsa, Optimization and Modeling of Cr (VI) Removal from Tannery Wastewater onto Activated Carbon Prepared from Coffee Husk and Sulfuric Acid (H 2 SO 4) as Activating Agent by Using Central Composite Design (CCD), 2023, p. 2023.

[77] D.L. Pavia, G.M. Lampman, G.S. Kriz, J.A. Vyvyan, 11 introduction to spectroscopy, in: Org. Chem, De Gruyter, 2022, pp. 205–236, https://doi.org/10.1515/9783110778311-011.

[78] H.-J. Kunze, Introduction to Plasma Spectroscopy, Springer Berlin Heidelberg, Berlin, Heidelberg, 2009, https://doi.org/10.1007/978-3-642-02233-3.

[79] A. Hariharan, V. Harini, S. Sandhya, S. Rangabhashiyam, Waste Musa acuminata residue as a potential biosorbent for the removal of hexavalent chromium from synthetic wastewater, Biomass Convers. Biorefinery 13 (2020) 1297–1310, https://doi.org/10.1007/s13399-020-01173-3.

[80] S. Hadi, E. Taheri, M.M. Amin, A. Fatehizadeh, E.C. Lima, Fabrication of activated carbon from pomegranate husk by dual consecutive chemical activation for 4-chlorophenol adsorption, Environ. Sci. Pollut. Res. 28 (2021) 13919–13930, https://doi.org/10.1007/s11356-020-11624-z.

[81] C. Patra, T. Shahnaz, S. Subbiah, S. Narayanasamy, Comparative assessment of raw and acid-activated preparations of novel Pongamia pinnata shells for adsorption of hexavalent chromium from simulated wastewater, Environ. Sci. Pollut. Res. 27 (2020) 14836–14851, https://doi.org/10.1007/s11356-020-07979-y.

[82] A.A. Oyekanmi, A. Ahmad, K. Hossain, M. Rafatullah, Adsorption of Rhodamine B dye from aqueous solution onto acid treated banana peel: response surface methodology, kinetics and isotherm studies, PLoS One 14 (2019) 216878, https://doi.org/10.1371/journal.pone.0216878.

[83] S. Fang, X. Huang, S. Xie, J. Du, J. Zhu, K. Wang, Q. Zhuang, X. Huang, Removal of chromium (VI) by a magnetic nanoscale zerovalent iron–assisted chicken manure-derived biochar: adsorption behavior and synergetic mechanism, Front. Bioeng. Biotechnol. 10 (2022), https://doi.org/10.3389/fbioe.2022.935525.

[84] O.K. Akiode, A. Adetoro, A.I. Anene, S.O. Afolabi, Y.A. Alli, Methodical study of chromium (VI) ion adsorption from aqueous solution using low-cost agro-waste material: isotherm, kinetic, and thermodynamic studies, Environ. Sci. Pollut. Res. 30 (2023) 48036–48047, https://doi.org/10.1007/s11356-023-25706-1.

[85] C. Xu, W. Yang, W. Liu, H. Sun, C. Jiao, A. Lin, Performance and mechanism of Cr (VI) removal by zero-valent iron loaded onto expanded graphite, J. Environ. Sci. 67 (2018) 14–22, https://doi.org/10.1016/j.jes.2017.11.003.

[86] A.A. Khan, S. Mukherjee, M. Mondal, S. Boddu, T. Subbaiah, G. Halder, Assessment of algal biomass towards removal of Cr(VI) from tannery effluent: a sustainable approach, Environ. Sci. Pollut. Res. 29 (2022) 61856–61869, https://doi.org/10.1007/s11356-021-16102-8.

[87] T.S. Badessa, E. Wakuma, A.M. Yimer, Bio-sorption for effective removal of chromium(VI) from wastewater using Moringa stenopetala seed powder (MSSP) and banana peel powder (BPP), BMC Chem. 14 (2020) 71, https://doi.org/10.1186/s13065-020-00724-z.

[88] N.K. Mondal, A. Samanta, S. Chakraborty, W.A. Shaikh, Enhanced chromium (VI) removal using banana peel dust: isotherms, kinetics and thermodynamics study, Sustain. Water Resour. Manag. 4 (2018) 489–497, https://doi.org/10.1007/s40899-017-0130-7.

[89] A.K. Chauhan, N. Kataria, R. Gupta, V.K. Garg, Biogenic fabrication of ZnO@ EC and MgO@ EC using Eucalyptus leaf extract for the removal of hexavalent chromium Cr (VI) ions from water, Environ. Sci. Pollut. Res. 30 (2023) 1–18, https://doi.org/10.1007/s11356-022-24967-6.

[90] R. Kumar, D.K. Arya, N. Singh, H.K. Vats, Removal of Cr (VI) using low cost activated carbon developed by agricultural waste, IOSR J. Appl. Chem. 10 (2017) 76–79, https://doi.org/10.9790/5736-1001017679.

[91] U. Maheshwari, S. Gupta, Removal of Cr(VI) from wastewater using a natural nanoporous adsorbent: experimental, kinetic and optimization studies, Adsorpt. Sci. Technol. 33 (2015) 71–88, https://doi.org/10.1260/0263-6174.33.1.71.

[92] S. Rangabhashiyam, E. Nakkeeran, N. Anu, N. Selvaraju, Biosorption potential of a novel powder, prepared from Ficus auriculata leaves, for sequestration of hexavalent chromium from aqueous solutions, Res. Chem. Intermed. 41 (2015) 8405–8424, https://doi.org/10.1007/s11164-014-1900-6.

[93] E. Ben Khalifa, S. Azaiez, G. Magnacca, F. Cesano, P. Benzi, B. Hamrouni, Synthesis and characterization of promising biochars for hexavalent chromium removal: application of response surface methodology approach, Int. J. Environ. Sci. Technol. 20 (2023) 4111–4126, https://doi.org/10.1007/s13762-022-04270-0.

[94] G.K. Gupta, M. Ram, R. Bala, M. Kapur, M.K. Mondal, Pyrolysis of chemically treated corncob for biochar production and its application in Cr(VI) removal, Environ. Prog. Sustain. Energy 37 (2018) 1606–1617, https://doi.org/10.1002/ep.12838.

[95] J. Bayuo, M.A. Abukari, K.B. Pelig-Ba, Optimization using central composite design (CCD) of response surface methodology (RSM) for biosorption of hexavalent chromium from aqueous media, Appl. Water Sci. 10 (2020) 135, https://doi.org/10.1007/s13201-020-01213-3.

[96] S. Afshin, Y. Rashtbari, M. Vosough, A. Dargahi, M. Fazlzadeh, A. Behzad, M. Yousefi, Application of Box–Behnken design for optimizing parameters of hexavalent chromium removal from aqueous solutions using Fe3O4 loaded on activated carbon prepared from alga: kinetics and equilibrium study, J. Water Process Eng. 42 (2021) 102113, https://doi.org/10.1016/j.jwpe.2021.102113.

[97] S. Sharifi, R. Nabizadeh, B. Akbarpour, A. Azari, H.R. Ghaffari, S. Nazmara, B. Mahmoudi, L. Shiri, M. Yousefi, Modeling and optimizing parameters affecting hexavalent chromium adsorption from aqueous solutions using Ti-XAD7 nanocomposite: RSM-CCD approach, kinetic, and isotherm studies, J. Environ. Heal. Sci. Eng. 17 (2019) 873–888, https://doi.org/10.1007/s40201-019-00405-7.

[98] R. He, X. Yuan, Z. Huang, H. Wang, L. Jiang, J. Huang, M. Tan, H. Li, Activated biochar with iron-loading and its application in removing Cr (VI) from aqueous solution, Colloids Surfaces A Physicochem. Eng. Asp. 579 (2019) 123642, https://doi.org/10.1016/j.colsurfa.2019.123642.

[99] A. Herath, C. Reid, F. Perez, C.U. Pittman, T.E. Mlsna, Biochar-supported polyaniline hybrid for aqueous chromium and nitrate adsorption, J. Environ. Manage. 296 (2021) 113186, https://doi.org/10.1016/j.jenvman.2021.113186.

[100] E.A. Ashour, M.A. Tony, Eco-friendly removal of hexavalent chromium from aqueous solution using natural clay mineral: activation and modification effects, SN Appl. Sci. 2 (2020) 2042, https://doi.org/10.1007/s42452-020-03873-x.

[101] H. Ma, J. Yang, X. Gao, Z. Liu, X. Liu, Z. Xu, Removal of chromium (VI) from water by porous carbon derived from corn straw: influencing factors, regeneration and mechanism, J. Hazard Mater. 369 (2019) 550–560, https://doi.org/10.1016/j.jhazmat.2019.02.063.